JOURNAL OF MATERIALS SCIENCE 30 (1995) 5732–5736

Kinetic studies of the glass transition in $(Se_{65}Te_{35})_{100-x}Sb_x$ by differential scanning calorimetry

M.MEHDI, G.BRUN, J. C. JUMAS, J. C. TEDENAC
Laboratoire de Physicochimie des Materiaux Solides, URA D0407, Université de Montpellier II, Sciences et Techniques du Languedoc, 34095 Montpellier cedex 05, France

Calorimetric studies of chalcogenide glasses, $(Se_{65}T_{35})_{100-x}Sb_x$, obtained by ice–water quenching, were performed by a non-isothermal method. An X-ray diffraction study, as a function of temperature, was carried out, with samples of different compositions. The activation energy for relaxation time, was determined from the heating-rate dependence of values of the glass transition temperature, as a function of x. A maximum in ΔE_t versus antimony concentration occurs at 1–2 at %. ^{121}Sb Mössbauer results confirm the formation of Sb_2Se_3, by crystallization.

1. Introduction

Se–Te alloys are very important materials for use as photoreceptors in the xerography process. Se–Te alloys are widely used because they have a high photosensitivity and a higher wear resistance than pure selenium. They have, however, shortcomings, such as a large residual potential which is induced after several charge–discharge cycles and a thermal instability, that is, the possibility of crystallization, which shortens the lifetime of photoreceptors. They have been doped with antimony in order to improve the thermal stability and the electrophotographic properties.

Furthermore it has been found that the Se–Te–Sb system shows memory-type switching and that the structure and electrical properties of glasses are considerably modified by the addition of antimony [1, 2]. So far, results concerning either the glass transition as a function of composition or crystallization kinetics are contradictory, and the structural explanations only approximate [3, 4]. For example, it is difficult to determine what changes have occurred in the antimony environment between the crystallization and melting temperatures.

Our aim in the present work was to clarify such questions in giving X-ray diffraction, glass transition and Mössbauer spectroscopy results. Crystallization kinetics will be reported elsewhere [5].

2. Experimental procedure

Homogeneous specimens of glassy $(Se_{65}Te_{35})_{100-x}Sb_x$, with $0 \leqslant x \leqslant 10$, were prepared by heating suitable amounts of 99.999% pure materials sealed in quartz ampoules under a vacuum of 10^{-5} torr (1 torr = 133.322 Pa) to 600 °C for 24 h. The melt was periodically shaken to ensure homogeneity and to avoid bubble formation. The ampoule was quenched in ice–water. The amorphous nature of the alloys was confirmed by X-ray diffraction. The glasses thus prepared were ground to fine powder for differential scanning calorimetry (DSC) studies. Amounts of powdered sample (40–50 mg) were placed in closed aluminium pans and then heated at a constant heating rate while thermograms were recorded using Setaram DSC 121 thermal analyser. Different heating rates (1, 2.5, 5, 10, 20 and 30 K min^{-1}) were chosen to study the heating-rate dependence of glass transition, and crystallization temperatures. Small quartz ampoules sealed under vacuum were used when melting conditions were to be reached. All the runs were performed under an argon atmosphere.

The ^{121}Sb Mössbauer spectroscopy was performed with a $Ca(^{121m}Sn)SbO_3$ source and absorber at the helium temperature using a cooling equipment, and a spectrometer Elscint AME40 coupled with a scanner Promeda 01. Each absorber containing 30 mg cm^{-2} ^{121}Sb was prepared by carefully mixing the powdered sample with silicone grease and enclosing the mixture between aluminium sheets in a copper holder.

3. Glass–crystal transition by X-ray diffraction

An X-ray study as a function of temperature was carried out with samples of different compositions. Fig. 1 shows the results obtained with the glass of $Se_{65}Te_{35}$ composition. The temperature intervals are 5 °C; each equilibrium setting and registration takes about 20 min. It is considered that the heating rate is extremely slow and that the system is always close to equilibrium. The glass–crystal transition is clearly visible. For the higher values of x (antimony-rich samples) the X-ray diffractogram shows essentially peaks

0022–2461

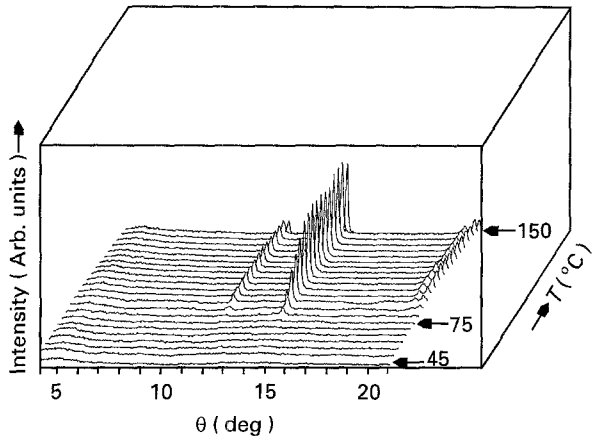

Figure 1 X-ray diffractogram of the $Se_{65}Te_{35}$ sample as a function of temperature.

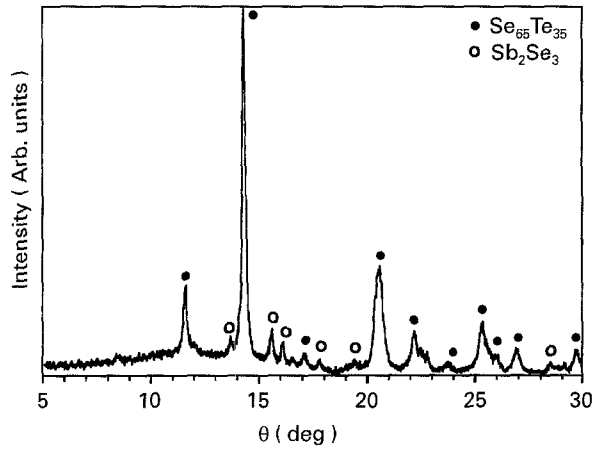

Figure 2 X-ray diffraction of $(Se_{65}Te_{35})_{90}Sb_{10}$ annealed at 150 °C for a few hours.

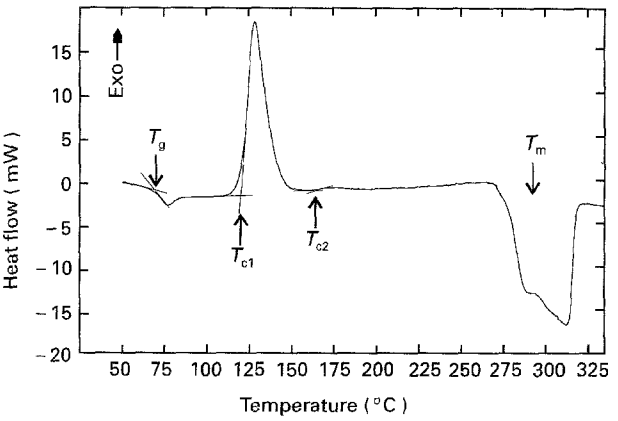

Figure 3 Typical DSC thermogram for $(Se_{65}Te_{35})_{94}Sb_6$ at heating rate of 2 K min^{-1}.

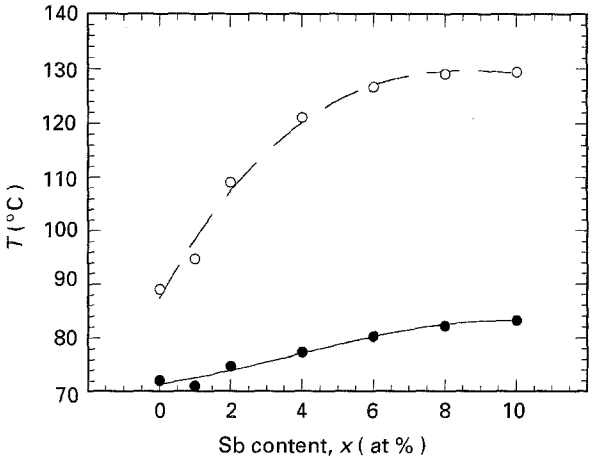

Figure 4 Composition dependence of (●) the glass transition temperature and (○) the crystallization peak temperature as a function of at % Sb at a heating rate of 5 K min^{-1}.

corresponding to the Se–Te solid-solution structure (hexagonal framework, cell parameters $a = 0.442$ nm, $c = 0.529$ nm). After few hours of annealing at 150° C, several new peaks of low intensity corresponding to the compound Sb_2Se_3 appear (Fig. 2). This is in agreement with the equilibrium phase diagram of the Se–Sb–Te system [6]. The compositions under study belong to the triangle Se–Te–Sb_2Se_3 and the crystallized solids at equilibrium at room temperature are indeed Sb_2Se_3 and the solid solution Se–Te.

4. DSC glass transition results

A typical DSC thermogram is shown in Fig. 3 for a sample of $(Se_{65}Te_{35})_{94}Sb_6$ composition, sealed in a silica tube (180 mg) and heated at $\alpha = 2$ K min^{-1}. Similar results to those shown in Fig. 3 have been obtained for all the compositions (x values) at different heating rates, α. T_g was taken as the temperature corresponding to the inflexion point in the rapidly rising part of the heat capacity curve. It is clear from this figure that well-defined endothermic peaks are observed at the glass transition temperture, T_g, rather than a shift of the baseline. At a higher temperature, an exothermic peak which corresponds to the crystallization temperature, T_c, is then observed. The onset temperature of the melting peak, T_m, is quite constant (270–275 °C), whatever the antimony composition. The melting peak range goes up to about 320 °C with at least three maxima. It corresponds roughly to the two-phase part between the liquidus and solidus lines of the Se–Te solid solution equilibrium diagram.

If Fig. 3 is observed more closely a second exothermic peak of very low intensity is observed. It is spread over about 30° (onset = 160 °C, T_{c2}). This peak is only seen for the higher values of x ($x = 6, 8, 10$) and probably corresponds to the separate crystallization of Sb_2Se_3. When the DSC heating rate, α, is larger than 20 K min^{-1}, T_{c1} and T_{c2} thermal effects can no longer be separated on the curve.

Another consequence of the formation of Sb_2Se_3 is the complexity of the melting process of the sample with a three-phase stage (liquid + Se–Te solid + Sb_2Se_3) before complete melting, which explains the three maxima on the curve.

Fig. 4 shows T_g and T_{c1} values (Table I) as a function of composition for a heating rate of 5 K min^{-1}. The heating-rate dependence of the glass transition temperature is interpreted in terms of thermal relaxation phenomena. In this kinetic interpretation, the enthalpy of the glassy system at a particular

TABLE I Glass transition temperature, T_g, and crystallization temperature, T_{c1}, values as a function of composition, x, for a heating rate $\alpha = 5\ \mathrm{K\,min^{-1}}$

Compositions	T_g(°C)	T_c(°C)
$Se_{65}Te_{35}$	72.20	89.11
$(Se_{65}Te_{35})_{99}Sb_1$	71.20	94.80
$(Se_{65}Te_{35})_{98}Sb_2$	74.77	109.15
$(Se_{65}Te_{35})_{96}Sb_4$	77.38	121.25
$(Se_{65}Te_{35})_{94}Sb_6$	80.28	126.80
$(Se_{65}Te_{35})_{92}Sb_8$	82.22	129.15
$(Se_{65}Te_{35})_{90}Sb_{10}$	83.28	129.50

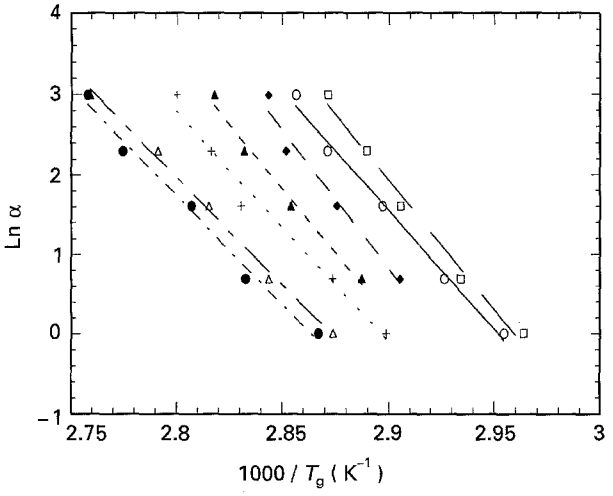

Figure 5 Heating rate, α, dependence of the glass transition temperature, for $x =$: (○) 0, (□) 1, (◆) 2, (▲) 4, (+) 6, (△) 8, (●) 10.

temperature and time, $H(t,T)$, relaxes isothermally, after an instantaneous change in temperature, towards a new equilibrium value $H_e(T)$. The relaxation equation can be written in the following form

$$(\partial H/\partial t)_T = -(H - H_e)/\tau \quad (1)$$

where τ is a temperature-dependent structural relaxation time and is given by the following relation

$$\tau = \tau_0 \exp(-\Delta E_t/(RT))\exp[-c(H - H_e)] \quad (2)$$

where τ_0 and c are constant and ΔE_t is the activation energy of the relaxation time. Using the above equations, it can be shown that

$$d\ln\alpha/d(1/T_g) = -\Delta E_t/R \quad (3)$$

α being the heating rate.

It is clear from (Equation 3) that the ln α versus $1/T_g$ plot should be a straight line and the activation energy involved around T_g can be calculated from the slope of this plot.

Fig. 5 shows ln α versus $10^3/T_g$ curves for various glasses in the $(Se_{65}Te_{35})_{100-x}Sb_x$ $(0 \leqslant x \leqslant 10)$ system. Such plots are found to be straight lines with an interval of error depending on the difficulty in appreciating the T_g value. Results are plotted as a function of antimony concentration in Fig. 6. It is clear from this figure that a maximum in ΔE_t versus antimony concentration occurs at 1–2 at %. The reason for this will

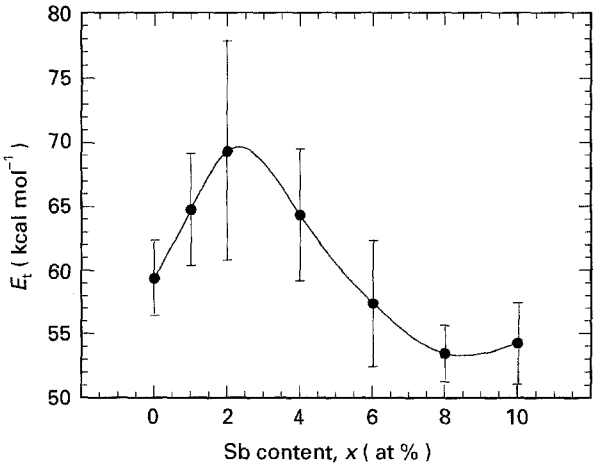

Figure 6 Composition dependence of the activation energy for thermal relaxation.

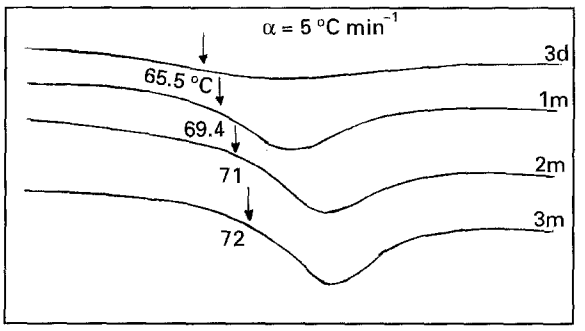

Figure 7 DSC heating scans of $(Se_{65}Te_{35})_{99}Sb$ glass after annealing at 25 °C for various times (3 days to 3 months)

TABLE II Glass transition temperature, T_g, and ΔC_p values as a function of relaxation time at room temperature for $(Se_{65}Te_{35})_{99}Sb$ and $\alpha = 5\ \mathrm{K\,min^{-1}}$

Times	T_g (°C)	ΔC_p (cal $g^{-1}\,°C^{-1}$)
3 days	65.5	0.087
1 month	69.4	0.146
2 months	71.0	0.212
3 months	72.0	0.212

be discussed later. The relaxation process involved to explain the heating-rate dependence of the glass transition is equally responsible for a reduction of T_g with time. Holding the samples at room temperature (near the glass transition temperature) for long times was found to be important to stabilize them [7]. That equilibrium state is finally achieved after 3–4 months. Fig. 7 shows DSC thermograms for a sample of composition $(Se_{65}Te_{35})_{99}Sb$, with a heating rate of $5\ \mathrm{K\,min^{-1}}$, around the glass transition, at different times (from 3 days to 3 months). A change and stabilization of ΔC_p is also observed (Table II). The T_g values reported in Fig. 4 have been measured on samples maintained 5 months at room temperature.

TABLE III ^{121}Sb Mössbauer parameters. δ = chemical isomer shift, Δ = quadrupole interaction, χ = degrees of freedom and MF = misfit

	δ^a (mm s^{-1})	Δ (mm s^{-1})	Γ (mm s^{-1})	χ^2	MF
$(Se_{65}Te_{35})_{98}Sb_2$ Glass	− 4.57	+ 9.6	1.45	0.963	0.158
$(Se_{65}Te_{35})_{90}Sb_{10}$ Glass	− 4.87 (3)	+ 9.5 (5)	1.50 (1)	1.27	0.28
$(Se_{65}Te_{35})_{98}Sb_2$ Crystallization with two sites[a]					
39.9%	− 5.15	+ 13.59	0.62	1.08	0.38
60.1%	− 5.95	+ 8.60			
$(Se_{65}Te_{35})_{92}Sb_8$ Crystallization with two sites[b]					
42.1%	− 4.70 (1)	+ 14.0 (1)	0.80 (1)	1.31	0.25
57.9%%	− 5.78 (9)	+ 9.5 (5)			
$(Se_{65}Te_{35})_{90}Sb_{10}$					
Crystallization	− 5.94 (2)	+ 7.48 (4)	1.43 (6)	1.35	0.016
Annealed	− 6.00 (2)	+ 7.36 (4)	1.44 (5)	1.04	0.19
Sb_2Se_3	− 6.15 (1)	+ 8.9 (3)	1.90 (6)	1.22	0.048

[a] Relative to InSb − 8.79(1)/Ca (^{121}Sm)SbO_3.
[b] DSC sample, heating process stopped before Sb_2Se_3 crystallization.

5. ^{121}Sb Mössbauer results

The ^{121}Sb Mössbauer data recorded from the $(Se_{65}Te_{35})_{100-x}Sb_x$ (with x = 2, 8, 10) are summarized in Table III.

A fitted Mössbauer spectrum for x = 8 is shown in Fig. 8. In all cases the Mössabauer spectra consisted of a single broad asymmetric peak which arises from an octet splitting through the electric field gradient.

The lines were not resolved. A single antimony site was assumed in the computational reduction of the data of glasses. A supposed double antimony site gave a better fitting of data of crystalline samples (x = 2 and 8). In the case of x = 8, the heating treatment of the sample was stopped before the Sb_2Se_3 crystallization peak occurs. Even in this case, part of the antimony atoms with a chemical isomer shift δ = − 5.78, not far from δ = − 6.14 (corresponding to Sb_2Se_3), is involved in the formation of this compound. This constitutes confirmation of DSC and XRD results. In spite of the $(Se_{65}Te_{35})$ matrix crystallization, the other part of the antimony atoms retains the glass characteristics (δ = − 4.70). Moreover, the quadrupole interaction is large and reflects a highly distorted environment for atoms still linked to the Se–Te chains. Similar results, though less clear owing to the smaller concentration of antimony atoms and the uncertainty in the position of the baseline, are obtained with the sample x = 2. Comparison between glass and crystallized sample (x = 10) results gives the best example of chemical isomer shift, from − 4.87 to − 6.00, indicating smaller binding, as expected, for the amorphous phase (and a weaker electronic density at the nucleus). In that case, all the antimony atoms appear as if they were linked as Sb_2Se_3 in the crystallized sample.

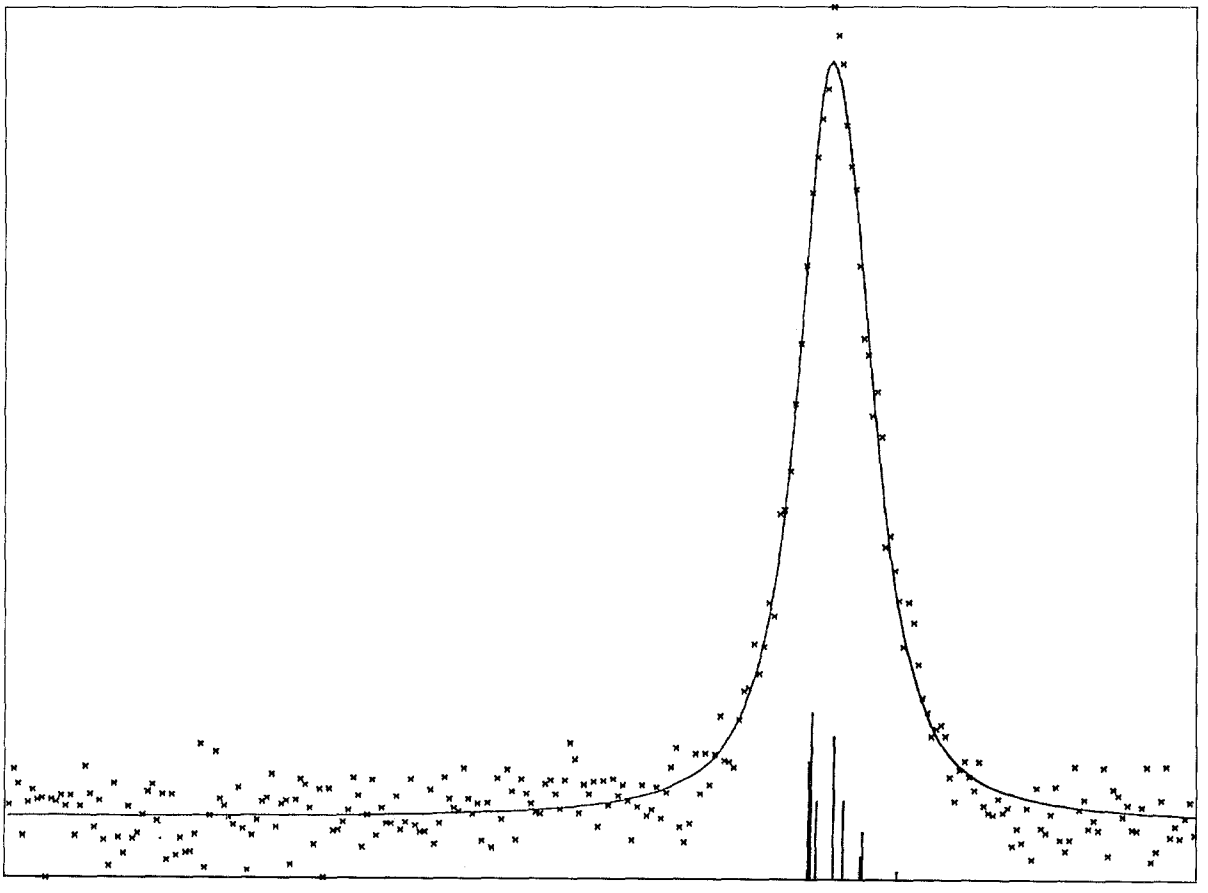

Figure 8 Antimony ^{121}Mössbauer spectra, recorded at 4 K, of $(Se_{65}Te_{35})_{92}Sb_8$.

6. Conclusion

Two important conclusions can be derived from these results. First, is the particular situation of the $x = 1$–2 composition, closely related to the hardening of the chain structure, which is probably due to the cross-linking by antimony atoms. That accounts for a higher value of activation energy of the glass transition. Second, the glass crystallization goes through a two-step process, particularly well shown either by XRD or by ^{121}Sb Mössbauer spectroscopy. The Se–Te matrix crystallizes first, including a few antimony atoms, tightly bonded, as defects. At 10–20 degrees temperature higher, Sb_2Se_3 phase is formed. Then it is important to note that a higher temperature is needed to melt it, mainly in the case of memory-switching application.

References

1. P. NAGELS, *Phys. Status Solidi (a)* **59** (1980) 505.
2. R. M. MEHRA, GURINDER, ASHTOSH GANJOO, RAVINDRA SINGH and P. C. MATHUR, *ibid.* **124** (1991) K51.
3. H.SAKAI, K. SHIMAKAWA, Y. INAGAKI and T. ARIZUMI, *J. Jpn Appl. Phys.* V **13**(3) (1974) 5.
4. R. M. MEHRA, G. KAUR and P. C. MATHUR, *J. Mater. Sci.* **26** (1991) 3433.
5. M. MEHDI, G. BRUN and J. C. TEDENAC, *ibid.* **30** (1995) 5259.
6. S. BORDAS, M. T. CLAVAGUERAMORA, B. LEGENDRE and C. HANCHENG, *Proceedings of 14th JEEP*, Montpelier, (1988) 139.
7. H. L. MA, X. H. ZLANG, J. LUCAS and C. T. MOYNIHAN, *J. Non-Cryst. Solids* **140** (1992) 209.

Received 27 May 1994
and accepted 28 April 1995